Observation of a Mott Insulating Ground State for Sn/Ge(111) at Low Temperature

R. Cortés,[1] A. Tejeda,[2] J. Lobo,[3] C. Didiot,[4] B. Kierren,[4] D. Malterre,[4] E. G. Michel,[5] and A. Mascaraque[1]

[1]*Departamento de Física de Materiales, Universidad Complutense de Madrid, 28040 Madrid, Spain*
[2]*Matériaux et Phénomènes Quantiques, UMR CNRS 7162, Université Paris 7, 75251 Paris, France*
[3]*Physik-Institut, University of Zurich and Swiss Light Source, Paul Scherrer Institut, Switzerland*
[4]*Laboratoire de Physique des Matériaux, Université Henri Poincaré, 54506 Vandouvre les Nancy, France*
[5]*Departamento de Física de la Materia Condensada, Universidad Autónoma de Madrid, 28049 Madrid, Spain*

(Received 27 December 2005; published 28 March 2006)

We report an investigation on the properties of 0.33 ML of Sn on Ge(111) at temperatures down to 5 K. Low-energy electron diffraction and scanning tunneling microscopy show that the (3×3) phase formed at $\sim$200 K, reverts to a new $(\sqrt{3} \times \sqrt{3})R30^\circ$ phase below 30 K. The vertical distortion characteristic of the (3×3) phase is lost across the phase transition, which is fully reversible. Angle-resolved photoemission experiments show that, concomitantly with the structural phase transition, a metal-insulator phase transition takes place. The $(\sqrt{3} \times \sqrt{3})R30^\circ$ ground state is interpreted as the formation of a Mott insulator for a narrow half-filled band in a two-dimensional triangular lattice.

DOI: 10.1103/PhysRevLett.96.126103 PACS numbers: 68.55.Jk, 68.37.Ef, 79.60.−i

The band theory of crystalline solids is one of the most successful parts of solid state physics. However, exceptions to the predictions of simple band theory are found when the approximation of independent electrons fails, due to electron repulsion effects [1]. This is the case of insulating materials that should be metallic according to band theory. In a simple view, the independent electron approach is not adequate when the kinetic energy (bandwidth) is smaller than the electron-electron interaction (Coulomb energy). The new ground state formed is the so-called Mott insulator [1]. It is characterized by strong electron-electron interactions, which are crucial to understand the behavior of many interesting materials [2].

Semiconductor surfaces present narrow surface bands, and thus are excellent playgrounds to search for Mott insulating phases, and to understand their rich physical behavior. Known examples of Mott insulators of this kind include the surfaces of SiC(0001) [3] and of K/Si(111):B [4]. In both cases, the occupation with adatoms of T_4 sites produces a $(\sqrt{3} \times \sqrt{3})R30^\circ$ structure ($\sqrt{3}$ in the following), which should exhibit a half-filled surface band, but is indeed insulating. The reconstructions of 0.33 monolayers (ML) of group IV adatoms on Si(111) or Ge(111) are isoelectronic with these systems and also exhibit the same atomic arrangement. Thus, they are good candidates to observe the same kind of behavior [5,6]. However, at variance with the two cases described above, the structure for both Sn and Pb on Ge(111) below $\sim$200 K is a (3×3) reconstruction [7,8]. This phase is metallic [9,10]. The (3×3) unit cell is distorted in a vertical direction because it contains three Sn adatoms and one of them is at a position higher ("up") than the other two ("down"). The different behavior in isoelectronic systems with such a similar atomic arrangement (Mott insulating vs metallic state), raises exciting issues on the origin of the different ground states found.

In this Letter, we demonstrate that the ground state of Sn/Ge(111) is a Mott insulating phase of $\sqrt{3}$ symmetry. We provide a full description of its structural and electronic properties by measuring at temperatures well below the values reached before. We find that below $\sim$30 K, the (3×3) phase becomes unstable and a new phase of $\sqrt{3}$ symmetry [11] is formed. The phase transition is fully reversible, and it is due to the disappearance of the (3×3) vertical distortion at low temperatures. Concomitantly with the structural phase transition, a band gap opens in the low-temperature, flat $\sqrt{3}$ phase. The Mott insulating phase competes with a metallic, (3×3) distorted state, which is more stable at higher temperatures.

The experiments were carried out in two different ultrahigh vacuum chambers, and include angle-resolved photoemission spectroscopy (ARPES), low-energy electron diffraction (LEED), and scanning tunneling microscopy (STM) measurements of 0.33 ML of Sn atoms on Ge(111). These techniques provide complementary information on both the short-range (STM) and long-range (LEED) surface order, and on the electronic structure and the single-particle spectral function (ARPES). The STM apparatus was a low-temperature microscope (Omicron), which operated between 4.7 and 300 K. ARPES experiments down to 10 K used a Scienta SES-2002 electron analyzer and synchrotron light from the SIS beam line at the Swiss Light Source [12]. Both chambers were equipped with LEED. The substrate was n-type Ge(111) ($\rho = 0.4\ \Omega\,\mathrm{cm}$). The preparation of the sample and of the (3×3) phase have been described before [9].

A sharp (3×3) LEED pattern is observed at 130 K (Fig. 1). Below $\sim$30 K, the (3×3) superstructure spots weaken and the pattern becomes $\sqrt{3}$. The new pattern is also sharp and with low background. The phase transition is fully reversible. We refer to this new phase as low-temperature $\sqrt{3}$ (LT $-\sqrt{3}$) [11].

© 2006 The American Physical Society

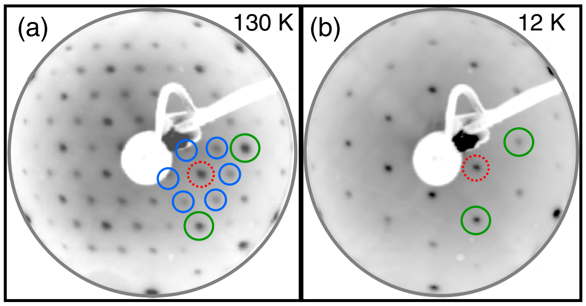

FIG. 1 (color online). LEED patterns from (a) the (3×3) and (b) the LT $-\sqrt{3}$ phase. The primary energy is 94 eV. Circles highlight (1×1) (green, large), (3×3) (blue, small), and $\sqrt{3}$ (red, dashed) spots.

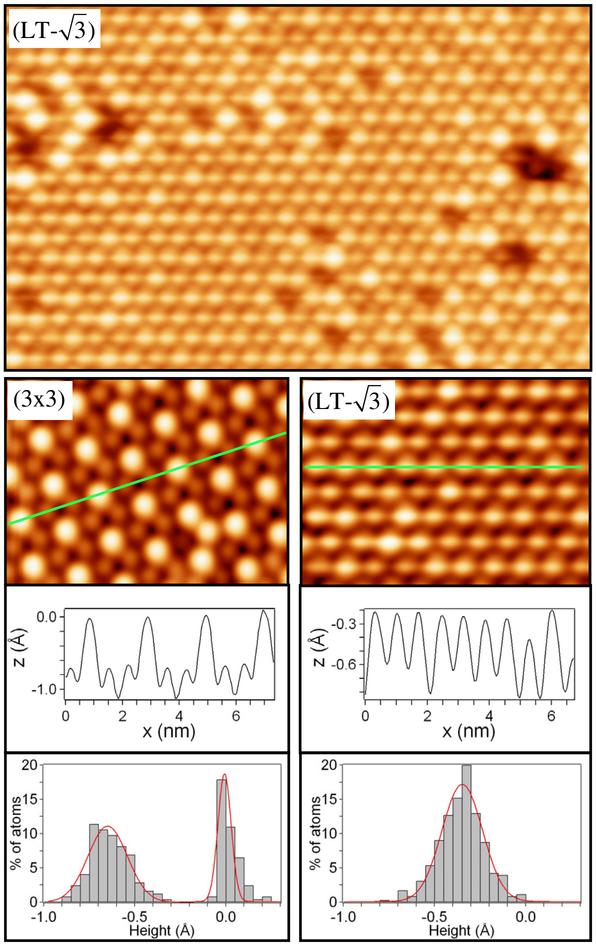

FIG. 2 (color online). Top: $18 \times 11\ \mathrm{nm}^2$ STM image ($V = -1.4$ V, $I = 1.0$ nA, $T = 5$ K) of the LT $-\sqrt{3}$ phase. Bottom: $7 \times 5\ \mathrm{nm}^2$ STM image of the (3×3) ($V = -1.0$ V, $I = 1.0$ nA, $T = 112$ K) phase and LT $-\sqrt{3}$ ($V = -1.4$ V, $I = 1.0$ nA, $T = 5$ K), respectively. Below, we show directly extracted height profiles corresponding to the direction highlighted in the STM image, and a histogram of the atomic heights found in each case.

Figure 2 shows filled-states representative STM images for the LT $-\sqrt{3}$ phase. There is an excellent $\sqrt{3}$ long-range order, and only atoms around defects appear brighter, indicating a local pinning to a (3×3) symmetry. To make easier the comparison, images of the same size of a LT $-\sqrt{3}$ and (3×3) surface are also shown. In the latter, the larger protrusions correspond to the up atom of the reconstruction, and form a hexagonal pattern. The two down atoms are resolved and imaged as smaller protrusions.

In order to understand the nature of the LT $-\sqrt{3}$ phase, the first step is discarding any artifact in the STM images. Such effects have been reported for the low-temperature reconstructions of Si(100) [13], Ge(111) [14], and Pb/Ge(111) [15]. In agreement with previous studies on Ge(111) with a similar doping as our sample [14], we find tip-induced band bending effects when the sample is in depletion conditions (i.e., a positive sample voltage for our n-doped sample). For negative sample voltages, images were acquired for a variety of measuring conditions. We find no detectable effect of the tip for a range of voltages and tunneling current, from which we select a safe range of reliable measuring conditions of $V = 1.0$–1.5 V and $I \leq 1$ nA. In conclusion, the loss of the (3×3) long-range order observed in LEED is explained from the disappearance of the atomic vertical distortion of the (3×3) phase, as observed in STM images. These structural modifications are fully reversible going up and down with temperature. Thus, the structure of the LT $-\sqrt{3}$ phase corresponds to the occupation of equivalent T_4 sites.

This finding is analyzed quantitatively in Fig. 2, which shows a height analysis for both the (3×3) and the LT $-\sqrt{3}$ phases. Atomic heights are measured for both reconstructions for 250 and 350 atoms, respectively. The results are shown as histograms in Fig. 2. Two different, well-defined heights are found for the (3×3) phase. The height difference is 0.65 Å. The height distribution is fit using two Gaussian functions. The height of up atoms is taken as zero level. An analogous height analysis for the LT $-\sqrt{3}$ phase shows that there is a single atomic height, following a Gaussian distribution. As mentioned above, atoms at distorted up positions survive around defects also for the LT $-\sqrt{3}$ phase. The location and relative height of these atoms has been monitored across the phase transition. We find that their atomic height does not change, and that they become part of the (3×3) reconstruction, once the phase transition is completed. Thus, their atomic height can be used to compare the atomic heights found for the LT $-\sqrt{3}$ and the (3×3) phases. Using this method, we find that the atomic height corresponding to the LT $-\sqrt{3}$ phase is 0.35 Å, between the heights of the up and down atoms of the (3×3) phase.

A crucial point to understand the nature of the LT $-\sqrt{3}$ phase is to analyze its electronic structure with ARPES. When ARPES is used to probe metal-semiconductor interfaces, surface photovoltage (SPV) effects should be taken into account [16,17]. UV radiation stabilizes a temperature-dependent SPV, which shifts uniformly both

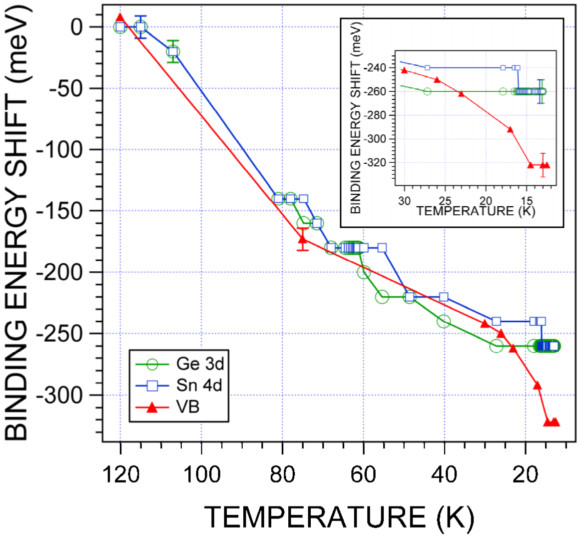

FIG. 3 (color online). Binding energy shift of Ge 3*d* (circles), Sn 4*d* (squares), and valence band leading edge (filled triangles) vs temperature. Values at 120 K are taken as a reference. Inset: enlarged view of the behavior for $T < 30$ K. Lines are a guide to the eye.

the core levels binding energies and the valence band. As expected for an *n*-doped sample, the three signals probed (Ge 3*d*, Sn 4*d*, and valence band leading edge) shift uniformly at low temperature to smaller values (Fig. 3). The value of the shift is the same for the three signals down to 30 K. The saturation of the shift at ~30 K for Ge 3*d* and Sn 4*d* indicates that "flat band conditions" are reached [18]. This situation corresponds to a complete elimination of the band bending [19], and thus no more shift is expected from the SPV effect. However, for temperatures below ~30 K, the binding energy of the valence band leading edge decreases further, deviating from the behavior of the core levels [20]. This additional shift reflects a depletion of the spectral intensity close to the Fermi energy (E_F), due to the opening of a surface band gap below 30 K. The energy difference below 15 K is 60 meV.

The opening of a surface band gap is confirmed by a detailed analysis with ARPES. Figure 4 shows the valence band along $[11\bar{2}]$ direction, which corresponds to $\overline{\Gamma\mathrm{M}}_{(3\times3)}$, for two different surface temperatures. The data are symmetrized with respect to E_F following standard practice in ARPES work on the cuprates [21]. In the symmetrized data, the effect of the Fermi function on the temperature dependence of the spectral function is removed. The position of E_F is corrected by the SPV, measured from the uniform shift of the Ge 3*d* and Sn 4*d* core levels. The value of E_F thus determined is in perfect agreement with the Fermi edge observed in the metallic (3×3) phase. The same method is used to determine E_F in the LT $- \sqrt{3}$ phase. Note the two surface state bands observed in the (3×3) phase, one of them crossing E_F. The spectral weight closer to E_F in the (3×3) phase disappears in the LT $- \sqrt{3}$ phase, indicating the opening of a surface band gap (Fig. 4). The depletion of spectral intensity around E_F affects a range of 0.4 eV below the valence band leading edge, and it gives rise to the apparent shift of the valence band detected below 30 K in Fig. 3. These changes are again fully reversible with temperature.

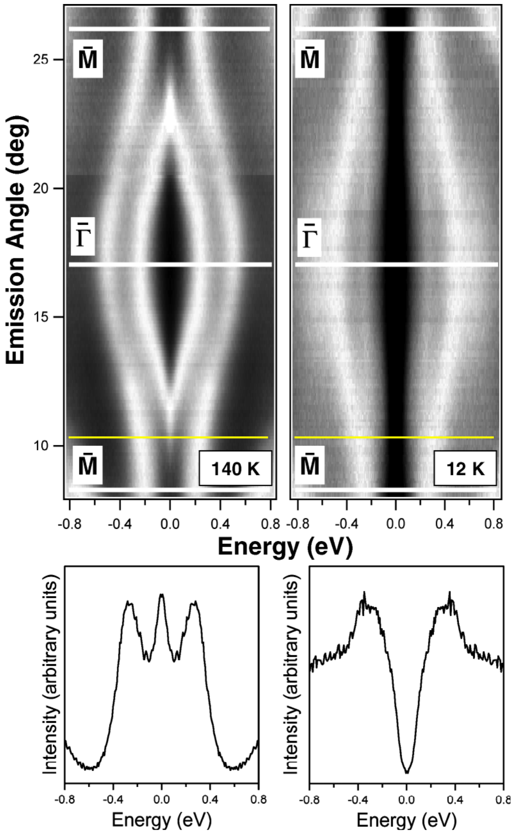

FIG. 4 (color online). Top: symmetrized angle-resolved photoemission spectra shown in gray scale (bright color means more intensity), as a function of emission angle along the $[11\bar{2}]$ direction for both the (3×3) (left) and the LT $- \sqrt{3}$ (right) phases. Symmetry points correspond to the (3×3) Brillouin zone. Bottom: two selected symmetrized spectra corresponding to the crossing point of the surface state (horizontal yellow line in top panel) at 140 (left) and 12 K (right). Energy scales are referred to E_F.

As shown in Fig. 4, the band gap and the corresponding redistribution of spectral intensity are fairly uniform, and they affect extended areas of reciprocal space. This is typical of a Mott insulator, where the band gap is not related to the surface periodicity, but rather to electron repulsion. These features of the electronic structure are qualitatively consistent with the spectral changes expected for a Mott transition [2,22,23]. The stabilization of a charge density wave by the Peierls mechanism would also give rise to a gap opening, but this possibility can be safely excluded because the surface Brillouin zone below 30 K is larger than above, at variance with the behavior expected for a Peierls distortion [24].

The existence of a Mott insulating ground state has been speculated from theoretical calculations performed in the local-density approximation (LDA), which have compared the stability of a flat $\sqrt{3}$ vs a distorted (3×3) structure. The ground state found was the (3×3) phase [9], but the energy difference with respect to a flat $\sqrt{3}$ phase was only 5 meV/Sn atom [5]. If electron correlation effects are considered, the energy difference between both phases would be even smaller, and close to the accuracy of the calculation, so we may expect that both phases are almost degenerate. It was also predicted that a flat $\sqrt{3}$ phase should become a Mott insulator [5]. The experiments show that both states are indeed observed. The energetic balance favors the (3×3) distorted metallic state above ~30 K, while the insulating, flat $\sqrt{3}$ phase is observed below this temperature. The existence of a phase transition indicates that there is a temperature-dependent modification of the potential energy landscape, by which electronic correlations become more important at low temperature. The stability of the (3×3) phase lies on a delicate balance between the electronic energy gained in the new structure and the elastic energy involved in the distortion [25], which affects not only the Sn atoms, but also several layers of the Ge(111) crystal [26]. We speculate that this feature is behind the phase transition observed, which might be triggered by two different mechanisms. On one hand, the elastic response of the lattice is effectively modified in Ge at low temperatures, as demonstrated by the negative lattice expansion and anomalous Grüneisen parameters below ~30 K [27]. This modification is due to a change of the phonon modes excited [28]. On the other hand, we expect that the charge screening is also modified at very low temperatures due to the decrease of the carrier concentration, favoring an increase of the effective electron repulsion. Any of these two effects may be strong enough to provoke the phase transition, but further work is needed to solve this open question, including theoretical calculations which take into account more accurately the role of electron correlations. Note also that recent reports provide contradictory evidence on the existence of a glassylike ground state for Pb/Ge(111) at low temperatures [15,29]. This disordered state is different from the $\sqrt{3}$ phase that we report here, which represents a well-ordered structure associated to a metal-insulator transition.

In conclusion, we present experimental evidence for a Mott insulating ground state of Sn/Ge(111). The results of three techniques (LEED, STM, and ARPES), which probe very different surface properties, converge to show that a structural phase transition from a distorted and metallic (3×3) phase to a flat and insulating $\mathrm{LT} - \sqrt{3}$ phase is observed at ~25 K. This finding is an indication of a more general phenomenon, which may also be observed in different metal-semiconductor interfaces.

We acknowledge financial support from MCyT (Spain) under Grants No. MAT2003-08627-C0201 and No. FIS2005-0747. A. M. thanks the program "Ramón y Cajal." R. C. thanks "Comunidad de Madrid" and "Fondo Social Europeo." Part of this work was performed at the Swiss Light Source, Paul Scherrer Institut, Villigen, Switzerland. STM images have been analyzed using WSxM software from Nanotec.

[1] F. Gebhard, *The Mott Metal-Insulator Transition* (Springer, New York, 1997).
[2] M. Imada, A. Fujimori, and Y. Tokura, Rev. Mod. Phys. **70**, 1039 (1998); M. Capone *et al.*, Phys. Rev. Lett. **93**, 047001 (2004); P. Limelette *et al.*, Science **302**, 89 (2003).
[3] L. I. Johansson, F. Owman, and P. Mårtensson, Surf. Sci. **360**, L478 (1996); J.-M. Themlin *et al.*, Europhys. Lett. **39**, 61 (1997).
[4] H. H. Weitering *et al.*, Phys. Rev. Lett. **78**, 1331 (1997).
[5] F. Flores *et al.*, Prog. Surf. Sci. **67**, 299 (2001).
[6] G. Santoro, S. Scandolo, and E. Tosatti, Phys. Rev. B **59**, 1891 (1999).
[7] J. M. Carpinelli *et al.*, Nature (London) **381**, 398 (1996); Phys. Rev. Lett. **79**, 2859 (1997).
[8] J. Ortega, R. Pérez, and F. Flores, J. Phys. Condens. Matter **14**, 5979 (2002) and references therein.
[9] J. Avila *et al.*, Phys. Rev. Lett. **82**, 442 (1999).
[10] R. I. G. Uhrberg and T. Balasubramanian, Phys. Rev. Lett. **81**, 2108 (1998).
[11] A $(\sqrt{3} \times 3)R30^\circ$ phase is also observed at room temperature, see Ref. [9].
[12] The energy/angle resolution is 9 meV/0.1°.
[13] S. Yoshida *et al.*, Phys. Rev. B **70**, 235411 (2004).
[14] R. M. Feenstra *et al.*, Phys. Rev. B **71**, 125316 (2005).
[15] I. Brihuega *et al.*, Phys. Rev. Lett. **95**, 206102 (2005).
[16] J. E. Demuth *et al.*, Phys. Rev. Lett. **56**, 1408 (1986).
[17] M. Alonso, R. Cimino, and K. Horn, Phys. Rev. Lett. **64**, 1947 (1990).
[18] The shift observed at 30 K is the maximum possible, as calculated from sample doping and the change of the chemical potential and of the Ge band gap with temperature.
[19] E. G. Michel *et al.*, Phys. Rev. B **45**, 11 811 (1992).
[20] A larger SPV for the valence band is discarded, first because the shift detected *exceeds* the maximum value due to a change of the band bending only, and second because the photon flux used for probing the core levels is larger than for the valence band.
[21] A. Damascelli, Z. Hussain, and Z. X. Shen, Rev. Mod. Phys. **75**, 473 (2003).
[22] L. Perfetti *et al.*, Phys. Rev. Lett. **90**, 166401 (2003).
[23] X. Y. Zhang, M. J. Rozenberg, and G. Kotliar, Phys. Rev. Lett. **70**, 1666 (1993).
[24] G. Grüner, *Density Waves in Solids* (Addison-Wesley, Reading, MA, 1994).
[25] D. Farias *et al.*, Phys. Rev. Lett. **91**, 016103 (2003).
[26] A. Mascaraque *et al.*, Phys. Rev. Lett. **82**, 2524 (1999).
[27] G. Dolling and R. A. Cowley, Proc. Phys. Soc. London **88**, 463 (1966).
[28] S. Biernacki and M. Scheffler, Phys. Rev. Lett. **63**, 290 (1989).
[29] J. Guo, J. Shi, and E. W. Plummer, Phys. Rev. Lett. **94**, 036105 (2005).